University of Twente

EEMCS / Electrical Engineering
Robotics and *Mechatronics*

Three-Dimensional Tracking of Magnetotactic Bacteria

B.A. (Bart) Reefman

Individual Assignment

Committee:
Dr. S. Misra
I.S.M. Khalil, PhD
Dr.ir. L. Abelmann

February 2013

Report nr. 002RAM2013
Robotics and Mechatronics
EE-Math-CS
University of Twente
P.O. Box 217
7500 AE Enschede
The Netherlands

Introduction

This thesis describes an algorithm to track and control magnetotactic bacteria (MTB). First, a model of the MTB is developed. Also the magnetic system used to control the MTB is modeled and verified. From this model, the applied magnetic field can be described as function of the current. Hereafter, a feature tracking algorithm for tracking of the MTB in two-dimensions is developed. This feature tracking algorithm is based on the subtraction of two consecutive image frames. In addition, the feature tracking algorithm is implemented to track the MTB in three-dimensional space. Calibration is done to track the MTB in three-dimensional space. The tracking algorithm is used in the realization of a closed-loop control system. This control system enables us to manipulate MTB.

The feature tracking algorithm enable us to track MTB inside a micro-fabricated maze with a channel width of 10 µm. The closed-loop control system can manipulate the MTB inside the micro-fabricated maze and position the MTB within a region-of-convergence of 10 µm in diameter. Further, the MTB can move at a velocity of 8 µm/s inside the maze. My contribution to this work is:

1. Verifying the model of the magnetic system by comparing measurements with simulated values
2. Development of a feature tracking algorithm, to track the MTB
3. Calibration of two videos and get the three-dimensional position of the MTB
4. Three-dimensional tracking of the MTB.

Three-Dimensional Tracking of Magnetotactic Bacteria

Bart A. Reefman*, Islam S. M. Khalil*, Leon Abelmann† and Sarthak Misra*

***Abstract*— This work addresses the tracking and control of magnetotactic bacteria (MTB) using a magnetic-based manipulation system. We present a technique to track the motion of MTB in the three-dimensional space. Our feature tracking algorithm is based on subtraction of the backgrounds of two input videos. These videos are provided by our three-dimensional magnetic system. This background subtraction allows the tracking algorithm to be insensitive to a variety of factors, such as lighting changes and perspective distortions. In addition, our feature tracking algorithm allows us to track MTB within a micro fabricated maze with a channel width of 10 μm. Our algorithm enables us to track MTB with an average length of 5 μm. A model of the electromagnetic system is developed and utilized in the realization of a control system. The motion control system allows the MTB to reach reference positions within the maze at a velocity of 8 μm/s and within a region-of-convergence of 10 μm in diameter. Furthermore, the tracking software provides a technique to track bacteria in the three-dimensional space.**

I. Introduction

A new promising development in healthcare is Minimal Invasive Surgery (MIS). Magnetotactic bacteria (MTB) can be utilized to carry out limited tasks such as targeted drug delivery [1]. Martel *et al.* demonstrated the open-loop control of a swarm of MTB to position microscopic structures. Using magnetotactic bacteria which are manipulated under the influence of applied magnetic fields, it becomes possible to perform manipulations at hard-to-reach locations. A system in which microrobots can be manipulated using 8 electromagnets is developed by Kummer *et al.* [2]. This magnetic system can position a 500 μm soft magnetic body using both open- and closed-loop control systems. A robust feature tracking algorithm is required for studying the behavior and control of the magnetotactic bacteria. Moreover, the MTB is shown in the inset in Fig. 1.Such a feature tracking algorithm is necessary for a closed-loop motion control system. Tracking of the *Escherichia Coli* bacteria with an adaptive kernel-based technique was done by Xie *et al.* [3]. Their algorithm allows tracking of multiple bacteria at a steady background. Open- and closed-loop control of MTB in two-dimensional (2D) space is demonstrated by Khalil *et al.* [4].

This paper provides a robust feature tracking algorithm in the three-dimensional (3D) space to track MTB. The tracking algorithm is insensitive to distortions such as exposure changes, background structures and image noise. This insensitivity is mainly caused by background subtraction. Some other techniques which are used in the feature tracking algorithm are thresholding, eroding and dilation. Increasing bandwidth is accomplished by a region of interest in which most of the image processing is done. In addition, a motion control system is implemented for the manipulation of MTB in the three-dimensional space. The motion control system uses the position of the MTB which is provided by our feature tracking algorithm. The feature tracking algorithm and motion control system are tested on the system showed in Fig. 1.

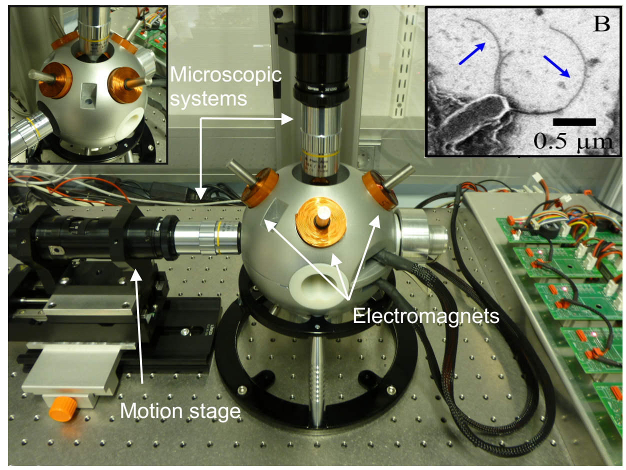

Fig. 1. Magnetic system for the wireless magnetic-based control of microparticles, microrobots and magnetotactic bacteria (MTB), i.e., *Magnetospirillum magnetotacticum*. The system is utilized to test the three-dimensional tracking and control of MTB. The MTB is shown in the top right inset, the blue arrows indicates the flagella of the MTB (images courtesy of Roel M.P. Metz and Marc P. Pichel).

The remainder of this paper is organized as follows: First the theoretical background pertaining to the modeling of magnetic forces, torque and drag forces is provided in Section II. In Section III, our feature tracking algorithm is presented. The control system of the MTB is provided in Section IV. The experimental results in two-dimensional space as well as tracking in three-dimensional space are provided in Section V. Finally, Section VI provides conclusions and directions for future work.

II. Theoretical Background

Considering a magnetic system with *n*-electromagnets for the manipulation of magnetic objects (microparticles, microrobots and magnetotactic bacteria). Using a microscopic system we are able to observe the motion of the microparticles, micro-robots and magnetotactic bacteria. In the

*Bart A. Reefman, Islam S. M. Khalil, and Sarthak Misra are with MIRA–Institute for Biomedical Technology and Technical Medicine, University of Twente, The Netherlands `b.a.reefman@student.utwente.nl`

†Leon Abelmann is with MESA+ Institute for Nanotechnology, University of Twente, The Netherlands

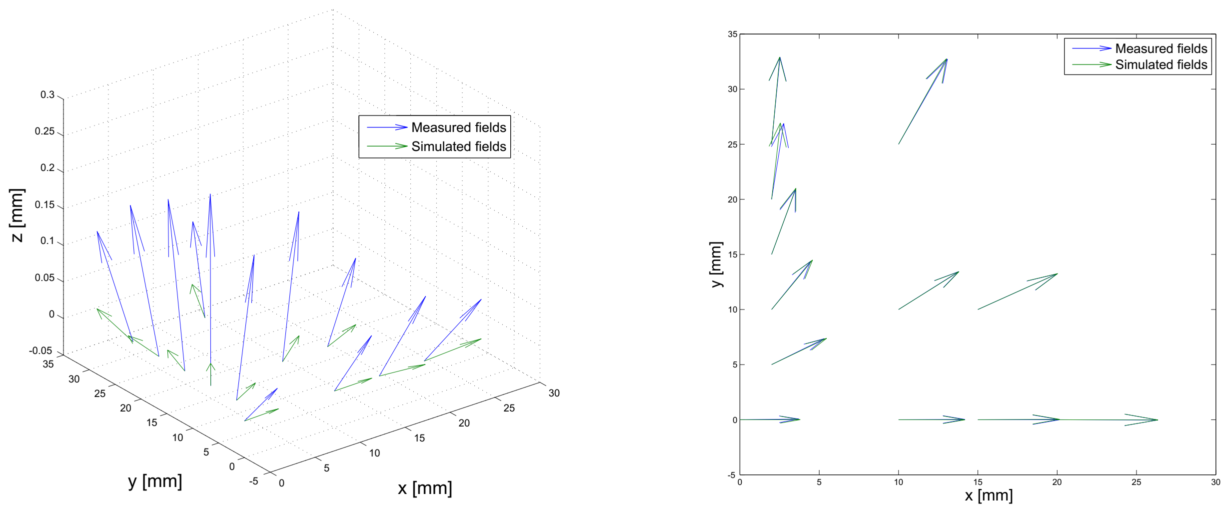

(a) Magnetic field measured and simulated in three dimensions

(b) Magnetic field measured and simulated displayed in x and y directions

Fig. 2. Comparison between measured and simulated magnetic fields around one side of a coil. Magnetic fields are measured using a 3-axis magnetometer (Sentron AG, Digital Teslameter 3MS1-A2D3-2-2T, Switzerland) . Simulated magnetic fields are generated by our Finite Element Model (FEM). In a three-dimensional plot (a) the deviations are large, but in a x y view (b) it becomes clear that there is only a deviation in z-direction. This deviation is caused by measurement errors

next Section we will explain how we modeled the magnetic force and verified the magnetic field [4].

A. Modeling of the Magnetotactic Bacteria

Under the influence of a magnetic field, the magnetic force $\left(\mathbf{F}\left(\mathbf{P}\right) \in \mathbb{R}^{3\times 1}\right)$ and torque $\left(\mathbf{T}\left(\mathbf{P}\right) \in \mathbb{R}^{3\times 1}\right)$ experienced by an MTB, i.e., *Magnetospirillum magnetotacticum*, located at position $\left(\mathbf{P} \in \mathbb{R}^{3\times 1}\right)$ are given by

$$\mathbf{F}(\mathbf{P}) = (\mathbf{m}\cdot\nabla)\mathbf{B}(\mathbf{P}) \quad \text{and} \quad \mathbf{T}(\mathbf{P}) = \mathbf{m}\times\mathbf{B}(\mathbf{P}), \qquad (1)$$

where $\mathbf{m} \in \mathbb{R}^{3\times 1}$ and $\mathbf{B}(\mathbf{P}) \in \mathbb{R}^{3\times 1}$ are the magnetic dipole moment of the MTB and the induced magnetic field, respectively. The magnetic torque, magnetic force and propulsion force overcome the drag force (F_{d}) and torque (T_{d}), respectively, and are given by

$$F_{\mathrm{d}} = \gamma v \quad \text{and} \quad T_{\mathrm{d}} = \alpha\omega. \qquad (2)$$

In (2), v and ω are the linear and angular velocities of the MTB, respectively. Further, γ is the linear drag coefficient and is given by [5]

$$\gamma = 2\pi\eta L\left[\ln\left(\frac{2L}{d}\right) - 0.5\right]^{-1}, \qquad (3)$$

where η, L and d are the dynamic viscosity of the fluid, length and diameter of the MTB, respectively. Further, in (2), α is the rotational drag coefficient and is given by [6]

$$\alpha = \frac{\pi\eta L^3}{3}\left[\ln\left(\frac{L}{d}\right) + 0.92\left(\frac{d}{L}\right) - 0.662\right]^{-1}. \qquad (4)$$

During the wireless control of an MTB, magnetic-based manipulation systems are utilized [7]. We consider a magnetic system with n-electromagnets. The magnetic field can be determined by the superposition of the contribution of each of the electromagnets [2]

$$\mathbf{B}(\mathbf{P}) = \sum_{i=1}^{n}\mathbf{B}_i(\mathbf{P}), \qquad (5)$$

where $\mathbf{B}_i(\mathbf{P})$ is the induced magnetic field by the ith electromagnet. The magnetic field $(\mathbf{B}_i(\mathbf{P}))$ is linearly proportional to the current (I_i) of the ith electromagnet. Therefore, (5) can be rewritten as

$$\mathbf{B}(\mathbf{P}) = \sum_{i=1}^{n}\widetilde{\mathbf{B}}_i(\mathbf{P})I_i = \widetilde{\mathbf{B}}(\mathbf{P})\mathbf{I}. \qquad (6)$$

In (6), $\widetilde{\mathbf{B}}(\mathbf{P}) \in \mathbb{R}^{3\times n}$ is a matrix which depends on the position at which the magnetic field is evaluated, and $\mathbf{I} \in \mathbb{R}^{n\times 1}$ is a vector of the applied current. The magnetic field due to each electromagnet is related to the current input by $\widetilde{\mathbf{B}}_i(\mathbf{P})$. Substituting (6) in the magnetic force equation (1) yields

$$\mathbf{F}(\mathbf{P}) = (\mathbf{m}\cdot\nabla)\widetilde{\mathbf{B}}(\mathbf{P})\mathbf{I} = \mathbf{\Lambda}(\mathbf{m},\mathbf{P})\mathbf{I}, \qquad (7)$$

where $\mathbf{\Lambda}(\mathbf{m},\mathbf{P}) \in \mathbb{R}^{3\times n}$ is the actuation matrix which maps the input currents onto magnetic forces. This actuation matrix depends on the magnetic dipole moment of the MTB and its position. Realization of this map necessitates the characterization of the magnetic dipole moment, and the evaluation of the magnetic field gradients at the position of the MTB [4]. A finite element model (FEM) is developed to realize (7). A FEM allows to calculate the magnetic field on given positions around the coils. The developed FEM is verified by measuring the magnetic fields at the same points as the FEM. In Fig. 2 a plot is shown of measured and simulated positions, the vector represents the direction and

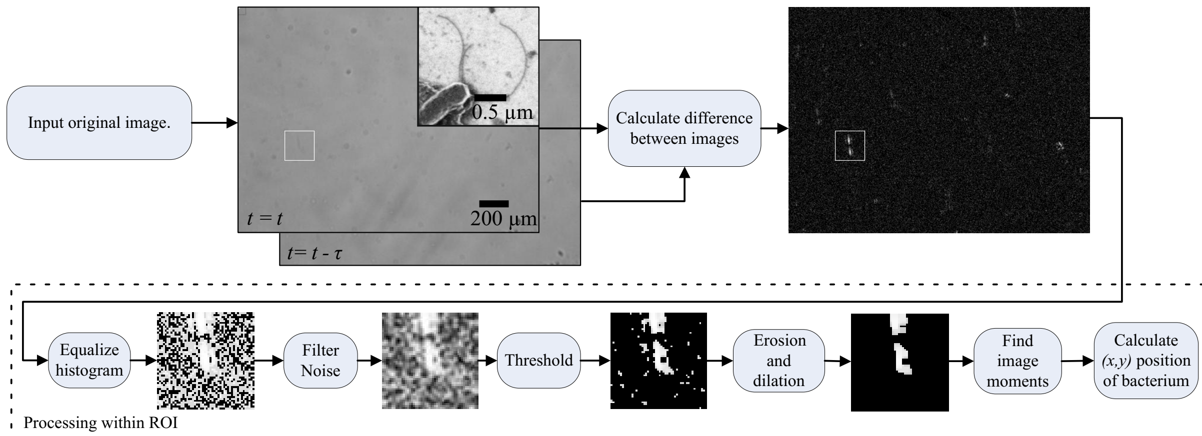

Fig. 3. Schematic view of the designed tracking algorithm, within the original image a region of interest (ROI) is located by selecting or by a known location of the bacterium, (MTB is shown in the top right inset). At time t the image is subtracted from the previous image. Further, τ is the time in seconds between two consecutive images. The ROI is subtracted from this image, here in Gaussian filtering, thresholding, erosion, dilation takes respectively place. Thresholding is in this image applied with a tresholdvalue of 201, where 0 represents a black pixel and 255 a white pixel. The location of the bacterium is found by calculating the image moments.

strength of the magnetic field at that point. As can be seen is the diversion in x- and y- direction minimal, there is only a large deviation in z-direction. This can be attributed to measurement errors. The simulated magnetic field can be imported in Matlab. This enables a surface fitting, with which the gradient of the magnetic field at a specific point **P** can be described in a third degree polynomial as a function of the x- and y-position of point (**P**). Calculating the gradient in z-direction at this point is done by interpolating between the different polynomials, in this way we are able to calculate the gradient in x, y and z direction at any point in space. The resulted formula's can be used for calculating the magnetic fields and thus the force on the bacteria at different points in space using equation (7) .

III. Feature Tracking Algorithm

Manipulating the MTB with a control system requires a model of the MTB and a robust feature tracking algorithm. The previous section provides a model of the MTB. In this section the feature tracking algorithm is provided, as well as the implementation of the two-dimensional tracking method in three-dimensional space.

A. Tracking Algorithm

Our feature tracking algorithm provides a method to track MTB in two- and three-dimensional space. Our algorithm also allows tracking of MTB in an image with background structures, such as 'walls' or static distortions. Tracking is achieved using the following steps (seen in Fig. 3).

1) *Background Subtraction:*

Filter background structures is done by a background subtractor.

$$\mathbf{I_d}(i,j) = \left|\mathbf{I_c}(i,j) - \mathbf{I_p}(i,j)\right|, \tag{8}$$

where $\mathbf{I_d}(i,j)$ is the intensity image as result of subtraction of the images $\mathbf{I_c}(i,j)$ and $\mathbf{I_p}(i,j)$ which are the current frame and the previous frame, respectively. The $|\cdot|$ operator provides the absolute value of $\mathbf{I_c}(i,j) - \mathbf{I_p}(i,j)$. Stationary features will have zero intensity because of this subtraction. We assume that the MTB is always moving, otherwise it will not be visible in $\mathbf{I_d}(i,j)$.

2) *Histogram Equalization:*

A larger contrast between bacteria and background is acquired by a histogram equalization [8]

$$\mathbf{I}(i,j) = 255\frac{(\mathbf{I_d}(i,j) - min(\mathbf{I_d}(i,j)))}{(max(\mathbf{I_d}(i,j)) - min(\mathbf{I_d}(i,j)))}, \tag{9}$$

where $\mathbf{I}(i,j)$ gives the maximum pixel value at position (i,j). Because the maximum pixelvalue can be 255, the histogram is spread between zero and 255. Moreover, $\mathbf{min}(\mathbf{I_d}(i,j))$ provides the lowest entry in the matrix $\mathbf{I_{diff}}$, whereas $\mathbf{max}(\mathbf{I_d}(i,j))$ provides the highest entry.

3) *Region Of Interest:*

A region of interest (ROI) is subtracted from the image after the image is equalized. A higher bandwidth is acquired by providing the ROI for the remaining image processing. The position of the ROI can be determined in two ways. First using the position which is provided by this tracking algorithm, after step 7. Knowing the position of the bacteria within the ROI, this should be transformed back to the position in the total image $(\mathbf{I}(i,j))$ The other method is selecting a ROI in the image, the mouse input position is then the new center of the ROI.

4) *First Noise Filter:*

In the ROI, the noise is filtered using a Gaussian blur filter [8].

5) *Image Thresholding:*

Thresholding provides a good manner to filter most of the noise. Thresholding works by

$$\mathbf{I_{th}}(i,j) = \begin{cases} \mathbf{I}(i,j) & \mathbf{I}(i,j) > \text{thresholdvalue} \\ 0 & \text{otherwise} \end{cases} \tag{10}$$

where $\mathbf{I_{th}}(i,j)$ is the image after thresholding. The $thresholdvalue$ can manually be adapted. This adaption ensures a more robust tracking algorithm since the lightning conditions can change between experiments. The initial value for the thresholdvalue is 201. The bacteria is always in motion therefore it will appear bright in the difference image, calculated in step 1. This fact implies that the thresholdvalue can be large.

6) *Image Erosion and Dilation:*
Thresholding does not filter all of the noise or small particles therefore erosion and dilation are applied respectively, both once. They are both applied using a standard 3×3 rectangular structuring element with the anchor at the element center [8].

7) *Image Moments:*
Now the only thing in the image are bacteria. By calculating the image moments the exact position of the bacterium can be determined using [9]. Using the new centroid position a new ROI can be subtracted of the new difference image.

B. Calibration and Three-Dimensional Tracking

Two cameras (camera 1 and camera 2) are necessary for tracking in 3D. Camera 1, the camera in the center in Fig. 1, is used for the x, y plane. The other, camera 2, the left camera in Fig. 1, is used for the x, z plane. Two videos on these planes a 3D image can be reconstructed. The two images must be related together via calibration. Therefore a 3D calibration is necessary. A micro-scale is used to perform calibration (Fig. 4). The dimensions of the scale are known beforehand. Therefore it can be used for calibration. By selecting 8 corresponding points in both images, coming from the 3D setup, the fundamental matrix ($\mathbf{F}$) can be estimated with a least square estimation algorithm and by using:

$$\mathbf{x_2}^T \mathbf{F} \mathbf{x_1} = 0, \tag{11}$$

where $\mathbf{x_1} \in \mathbb{R}^{3\times1}$ contains the coordinates of one point on the scale in the images of Camera 1. This image is used as basis for the coordinate system which are related by the fundamental matrix $\mathbf{F} \in \mathbb{R}^{3\times3}$. The matrix $\mathbf{x_2}$ contains the coordinates of the same point on the scale but in the other image coming from Camera 2, as explained in [10]. Using 8 corresponding points and the least median of squares method, $\mathbf{F}$ is determined. The epipolar lines ($\mathbf{l_1}$) and ($\mathbf{l_2}$) for Camera 1 and Camera 2 respectively, are given by

$$\mathbf{F}\mathbf{l_1} = \mathbf{0} \text{ and } \mathbf{F}^T\mathbf{l_2} = \mathbf{0}. \tag{12}$$

The camera matrix $\mathbf{C_1}$ for Camera 1 and the camera matrix $\mathbf{C_2}$ for Camera 2 are given by

$$\mathbf{C_1} = [\mathbf{\Pi}|\,\mathbf{0}] \text{ and } \mathbf{C_2} = [\mathbf{A}|\,\mathbf{a}], \tag{13}$$

where $\mathbf{\Pi} \in \mathbb{R}^{3\times3}$ is the identity matrix. Also the following relation for $\mathbf{A}$ and $\mathbf{a}$ is known:

$$\mathbf{a} = \mathbf{l_2} \text{ and } \mathbf{A}^{-1}\mathbf{a} = \mathbf{l}. \tag{14}$$

The set of camera-property matrices $\mathbf{A}$ and $\mathbf{a}$ can be used to calculate the camera matrices $\mathbf{C}$ and $\mathbf{C_2}$ via (13). These steps allows tracking of the MTB in three-dimensional space. The motion control system makes use of the provided feature tracking algorithm.

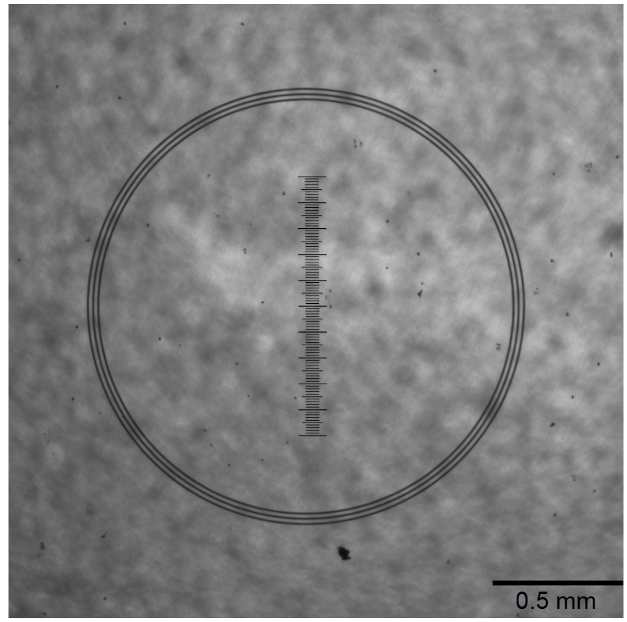

Fig. 4. The micrometer (Stage Micrometers, OBM1/100, Olympus Tokyo, Japan) used for the calibration. The circles are used to locate the scale under the microscope. The resolution of the scale is 10 μm.

IV. Closed-loop Control

Closed-loop control of an MTB is accomplished by directing the fields towards a reference position, then the MTB performs a flagellated swim towards this reference position. Due to the self-propulsion provided by the helical flagella, the closed-loop control action can only locate the MTB within the vicinity of the reference position [4].

A. Control System Design

In a low Reynolds number environment (inertial terms are ignored), motion of the MTB is governed by

$$\mid \mathbf{F}(\mathbf{P}) \mid + F_{\rm d} + f = 0 \quad \text{and} \quad \mid \mathbf{T}(\mathbf{P}) \mid + T_{\rm d} + \Omega = 0, \tag{15}$$

where f and Ω are the force and torque generated by each helical flagella, respectively. We use the force equation in (15), to generate the desired currents at each of the electromagnets. In order to realize the closed-loop control system, we calculate the position and velocity tracking errors as follows:

$$\mathbf{e} = \mathbf{P} - \mathbf{P_{ref}} \quad \text{and} \quad \dot{\mathbf{e}} = \dot{\mathbf{P}} - \dot{\mathbf{P}}_{\mathbf{ref}} = \dot{\mathbf{P}}. \tag{16}$$

In (16), $\mathbf{e}$ and $\dot{\mathbf{e}}$ are the position and velocity tracking errors, respectively. Further, $\mathbf{P_{ref}}$ is the fixed reference position. We devise a desired magnetic force ($\mathbf{F_{des}}(\mathbf{P})$) of the form

$$\mathbf{F_{des}}(\mathbf{P}) = \mathbf{K}_p\mathbf{e} + \mathbf{K}_d\dot{\mathbf{e}}, \tag{17}$$

where $\mathbf{K_p}$ and $\mathbf{K_d}$ are the controller positive-definite gain matrices and are given by

$$\mathbf{K_p} = \begin{bmatrix} k_{\mathrm{p}1} & 0 \\ 0 & k_{\mathrm{p}2} \end{bmatrix} \text{ and } \mathbf{K_d} = \begin{bmatrix} k_{\mathrm{d}1} & 0 \\ 0 & k_{\mathrm{d}2} \end{bmatrix}. \qquad (18)$$

In (18), $k_{\mathrm{p}i}$ and $k_{\mathrm{d}i}$, for $(i = 1, 2)$, are the proportional and derivative gains, respectively. Substitution of (17) in (15), i.e., $\mathbf{F_{des}}(\mathbf{P}) = \mathbf{F}(\mathbf{P})$, and assuming zero propulsion force $(f = 0)$ yields the following position tracking error dynamics:

$$\dot{\mathbf{e}} + (\mathbf{K_d} + \gamma \mathbf{I_2})^{-1} \mathbf{K_p} \mathbf{e} = 0, \qquad (19)$$

where $\mathbf{I_2} \in \mathbb{R}^{2\times 2}$ is the identity matrix.

B. Region of Convergence

Since motile MTB provides propulsion by its helical flagella, $f \neq 0$. Therefore, the closed-loop control system does not allow the position tracking error to go to zero, it rather locates the MTB within the vicinity of the reference position, i.e., region-of-convergence. Positioning accuracy of the control system can be evaluated by the diameter of the region-of-convergence. From (19), the size of the region-of-convergence depends on the gains of the control system, the propulsion force of the flagella and the dynamic viscosity of the fluid.

V. Experimental Results

Verifying the two- and three-dimensional tracking and control are done by experiments. Tracking and control are provided by using a three-dimensional magnetic system, with two microscopes which are placed orthogonally and on linear stages. These stages allows to use focusing and therefore track the bacteria in three-dimensional space. The magnetic system is shown in Fig. 1. Supplying a current to the coils produces a magnetic field, with this magnetic fields the microparticles, bacteria and microrobots can be manipulated. In this section the results of the experiments are provided. First of the two-dimensional tracking and hereafter the results of three-dimensional tracking. The algorithm assumes that there is only one bacterium in the ROI. If there are more than one bacterium in the ROI the image moments will change.

A. Two-Dimensional Tracking

We control the MTB inside the micro-fabricated maze (Fig. 6), to analyze the effect of the channel wall on the velocity and the positioning accuracy of the MTB. Fig. 6 provides the experimental result of the MTB inside the micro-fabricated maze. The feature tracking software enables the system to track the MTB even if it is in the surrounding of the walls. The control system (13) allows the MTB to follow two reference positions indicated by the small blue circles. We observe that the MTB is positioned within the vicinity of the reference positions and the region-of-convergence is 10 μm. The control system positions the MTB at a velocity of 8 μm/s.

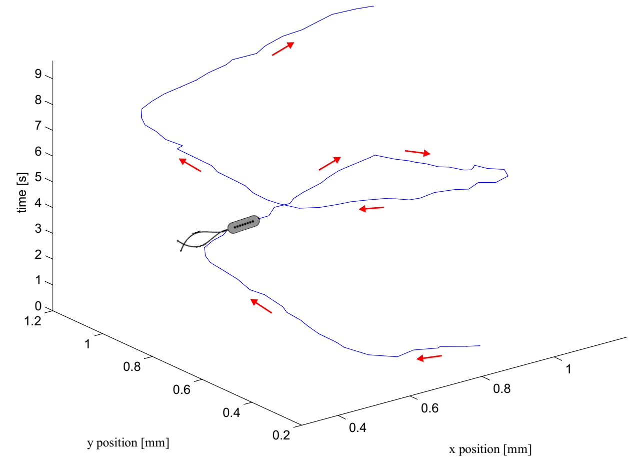

(a) Position of the magnetotactic bacterium.

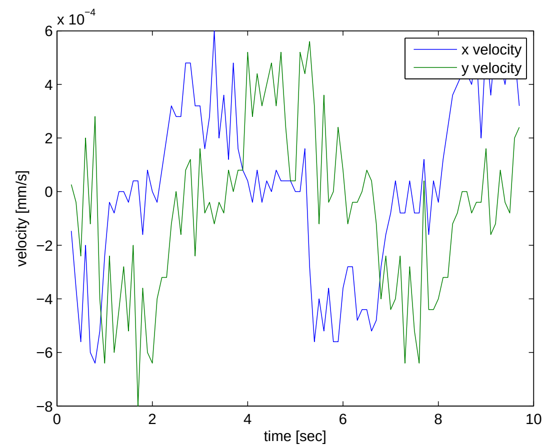

(b) Velocity of the magnetotactic bacterium along x- and y-axis during the rectangular trajectory.

Fig. 5. Tracking of the magnetotactic bacterium (MTB) in two-dimensions. The MTB follows a rectangular trajectory under the influence of uniform magnetic fields generated. Uniform fields are generated using a single electromagnet at a time as verified in Fig. 2, which is an open loop controller.

B. Three-Dimensional Tracking

Three-dimensional tracking is done in the same way as two-dimensional tracking. Linking both video's together is done by calibration. The results of three-dimensional tracking is showed in Fig. 7. Since the bacteria were non magnetic it was not possible to locate the same bacterium in both videos. Therefore the proof of concept is shown. We track two different bacteria at the same time.

VI. CONCLUSIONS AND RECOMMENDATIONS

This paper shows that it is possible to track magnetotactic bacteria within a micro-fabricated maze. The tracking is insensitive to a number of distortions such as occlusions, perspective distortions and intensity changes, to name just a few distortions. Moreover, it is also shown that the tracking is possible in three-dimensions.

Robustness is accomplished by calculating the differences between two frames, which filters out all static parts in the

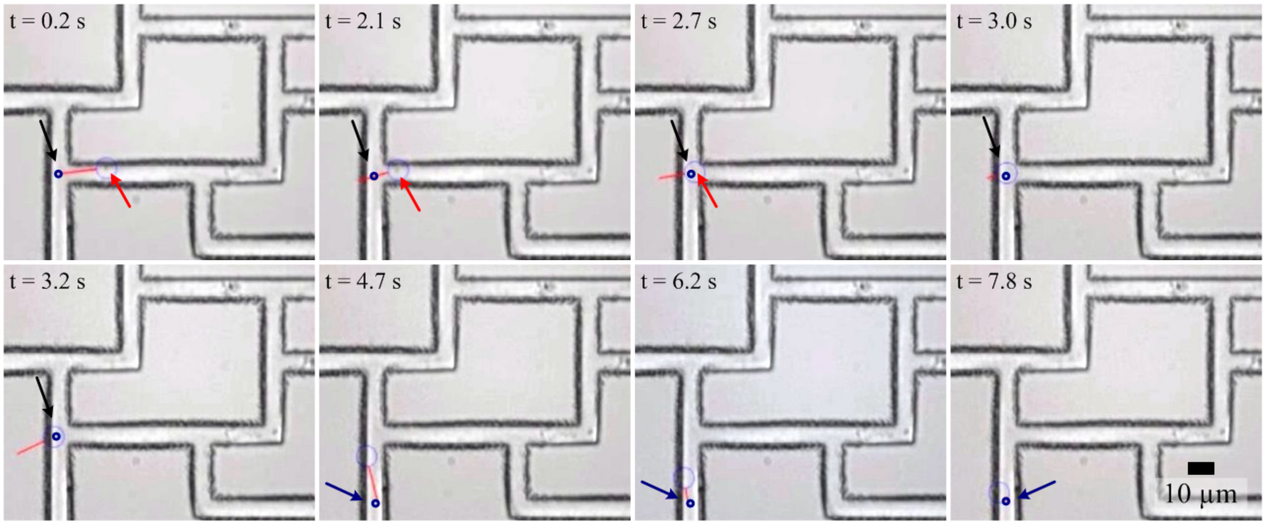

Fig. 6. Different time frames of the tracking and closed-loop control of a magnetotactic bacterium (MTB). The MTB is manipulated inside a microfabricated maze with an inner-width and -thickness of 10 μm and 5 μm. The MTB is positioned with a velocity of 8 μm/s within a region-of-convergence of 10 μm. These reference positions are indicated by the small blue circle. The large blue circle is the position of the MTB located by the provided tracking algorithm. A velocity vector of the MTB is represented by the red line, the red arrows indicate the controlled MTB.

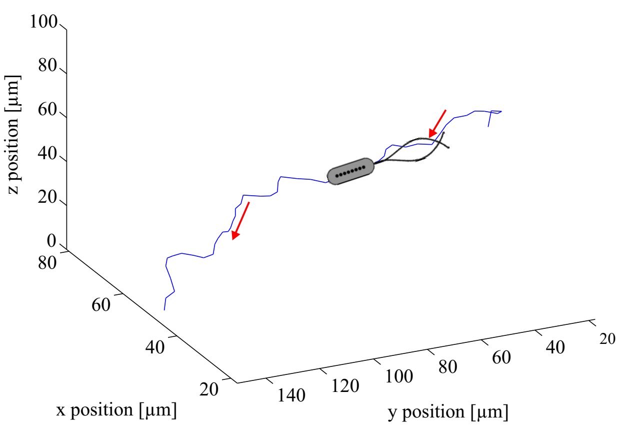

Fig. 7. Tracking of the magnetotactic bacterium (MTB) in three-dimensions. The MTB is swimming under the influence of the earth magnetic fields.

image. It is shown that this subtraction enables us to track bacteria in a maze-like structure.

The tracking also enables us to control the MTB in 3D. It is shown that due to the flagella force it is not possible to exactly position the bacteria. The bacteria can be positioned within a region of 10μm of the setpoint.

A. Future work

Improving the tracking algorithm can be done in several ways. To get it more robust, a way must be found to filter out most distortions as possible. This can be done be providing a cleaned microscopic system and a pure sample of bacteria. Furthermore, a Kalman predictor should be implemented as in [11] to predict the next position of the feature, which will become handy when the lightning changes or the bacterium is out of focus. The tracking can be of a higher bandwidth when subtracting the frames does not happen on the whole image but only on the ROI. By implementing autofocussing the tracking algorithm will be able to track MTB in 3D. Being able to do so also enables the control of MTB in 3D.

References

[1] S. Martel and M. Mohammadi, "Using a swarm of self-propelled natural microrobots in the form of flagellated bacteria to perform complex micro-assembly tasks," (Anchorage, Alaska), pp. 500–505, May 2010.

[2] M. P. Kummer *et al.*, "Octomag: an electromagnetic system for 5-dof wireless micromanipulation," *IEEE Transactions on Robotics*, vol. 26, pp. 1006–1017, 2010.

[3] J. Xie *et al.*, "Automatic tracking of escherichia coli bacteria," *Med. Image Computing and Computer-Assisted Intervention*, vol. 11, pp. 824–832, 2008.

[4] I. S. M. Khalil *et al.*, "Control of magnetotactic bacterium in a micro-fabricated maze," *Proc. IEEE Int'l. Conf. Robotics and Automation*, *in press*, 2013.

[5] H. C. Berg, *Random walks in biology*. Princeton, New Jersey: Princeton University Press., 1993.

[6] Y. R. Chemla *et al.*, "A new study of bacterial motion: superconducting quantum interference device microscopy of magnetotactic bacteria," *Biophysical Journal*, vol. 76, pp. 3323–3330, 1999.

[7] I. S. M. Khalil *et al.*, "Characterization and control biological mi-crorobots," in *Proceedings of the 13th international symposium on experimental robotics*, (Quebec, Canada), June 2012.

[8] F. van der Heijden, *Image based measurement systems: object recog-nition and parameter estimation*. Chichester, U.K.: John Wiley and Sons Ltd, 1994.

[9] J. D. Keuning *et al.*, "Image based magnetic control of paramagnetic microparticles in water," (San Francisco, USA), pp. 421–426, Septem-ber 2011.

[10] R. Hartley and A. Zisserman, *Multiple View Geometry in Computer Vision*. Cambridge, U.K.: Cambridge Univ. Press, 2000.

[11] G. Welch and G. Bishop, "An introduction to the kalman filter," in *SIGGRAPH 2001*, 2001.